# Estimation of Crown and Stem Water Content and Biomass of Boreal Forest Using Polarimetric SAR Imagery

**Sasan S. Saatchi and Mahta Moghaddam**
Jet Propulsion Laboratory, California Institute of Technology
4800 Oak Grove Drive, Pasadena, California 91109

Abstract. Characterization of boreal forests in ecosystem models requires temporal and spatial distributions of water content and biomass over local and regional scales. In this paper, we report on the use of a semi-empirical algorithm for deriving these parameters from polarimetric synthetic aperture radar measurements. The algorithm is based on a two layer radar backscatter model that stratifies the forest canopy into crown and stem layers and separates the structural and biometric attributes of forest stands. The structural parameters are estimated by training the model with SAR image data over dominant coniferous and deciduous stands in the boreal forest such as jack pine, black spruce, and aspen. The algorithm is then applied on AIRSAR images collected during the Boreal Ecosystem Atmospheric Study (BOREAS) over the boreal forest of Canada. The results are verified using biometry measurements during BOREAS intensive field campaigns. Field data relating the water content of tree components to dry biomass are used to modify the coefficients of the algorithm for crown and stem biomass. The algorithm was then applied over the entire image generating biomass maps. A set of 18 test sites within the imaged area was used to assess the accuracy of the biomass maps. The accuracy of biomass estimation is also investigated by choosing different combination of polarization and frequency channels of the AIRSAR system. It is shown that polarimetric data from P-band channels provide similar accuracy for estimating the above ground biomass for boreal forest types. In general, the use of P-band channels can provide better estimates of stem biomass while L-band channels can estimate the crown biomass more accurately. When AIRSAR image also used to simulate the data from existing spaceborne radar systems, it was found that the combination of L-band HH polarization (JERS-1), C-band HH polarization (RADARSAT), and C-band VV polarization (ERS-1) had limited capacity for mapping boreal biomass (63% accuracy).

# I. Introduction

There is an increasing interest in estimating forest biomass for both practical forestry applications, carbon sequestration credits, and other scientific applications such as modeling the land surface biochemical cycle. Biomass estimates are critical for studying the ecosystem structure and function and provide the means for assessing the timber value, forest productivity, regeneration, decomposition, and fire effects. As an environmental issue of global concern, the estimates of biomass will directly help to predict the increase of carbon dioxide in the atmosphere. The carbon dioxide flux as a result of land-use change and biomass removal or production are often derived from models that keep an account of the rates of carbon release and uptake. A source of error in these models is the uncertainty in the quantity of vegetation biomass over landscapes as an input parameter (Houghton, 1992).

Circumpolar boreal regions are particularly important because they may be the key regions for observing the impacts of global climate change. Recent results from Keeling et al.(1996) indicate an increase in the amplitude of the seasonal cycle of atmospheric $CO_2$, suggesting the lengthening of the growing season in the northern hemisphere, especially in higher latitudes. Other studies have also indicated that there might be significant warming and drying in the summer months in the same region and this may have an impact on the boreal forests being a sink or source of carbon (Davis and Botkin, 1985; Tans et al., 1990; ). These studies motivated the design of the BOREAS (boreal ecosystem-atmospheric study) project that started in 1993. One of the objectives of this project is to improve the status of process models that describe the exchanges of carbon and other trace gases between boreal forest and the atmosphere (Sellers et al., 1995). Applying these models over landscapes requires surface parameters such as land cover types and the above ground vegetation biomass (e.g. Running and Coughlan, 1988; Kimbal et al., 1999).

Although forest biomass has been identified as a crucial parameter in many studies, its determination has posed a nontrivial problem. Consider the data presented in Figure 1, which show two sets of measurements of biomass for the same homogeneous forest stands. The stands are all within the BOREAS study area. The first set, plotted on the vertical axis, was measured by Forestry Canada in 1993, and the second set, plotted on the horizontal axis, was measured by one of the BOREAS science teams during 1993-1996 field experiments (BOREAS information system, 1996). The 1:1 line (45-degree line) is drawn to facilitate the comparison between these measurements. For each stand, represented by the open circles, the standard deviation of each of the measurements is

shown. These data were obtained by measuring tree DBH (Diameter at 1.37 m height) and height in a limited number of plots (3 for Forestry Canada, and 4 for BOREAS) and allometric equations obtained from destructive sampling. The species types varied from stand to stand. The figure also shows that for the same stands there is often a large difference between the two measurements. The differences are as high as about 90 tons/ha. This effect is more pronounced for larger values of biomass, whereas for smaller values, i.e., less than 50 tons/ha, most measurements are close to the 1:1 line, or at least the error bars reach this line. For larger values of biomass, even the range defined by the error bars does not include this 1:1 line for many stands. The reason for such differences could be the number of plots, the location of the plots, spatial variability within each stand, size and weight measurement errors, and human errors. The first two of the above factors are deemed to be the most important ones, as they define the number of samples and hence the statistics of the measurements. The discrepancies are smaller for smaller biomass values, since typically there are a larger number of trees in each plot, and hence the biomass distribution can be better characterized. It is also important to note that the ground estimation of biomass becomes more difficult as the number of species within the stand increases such as in tropical forests (Brown and Lugo, 1990).

An alternate method of estimating biomass values has been through remote sensing measurements, in particular, those from airborne and spaceborne synthetic aperture radar (SAR) systems. In this category, the dominant methods have been variants of regression analyses, where a regression curve is fitted to a set of backscatter vs. ground-measured biomass values. This curve (usually a line) is then used over other areas and forest stands to obtain biomass for given radar backscatter. Although simple and practical, this approach is generally not valid if the forest type deviates from those used to obtain the regression curve (Le Toan et al., 1992; Hussin et al., 1991, Ranson and Sun, 1994, 1997; Dobson et al., 1995; Moghaddam et al., 1994; Rauste et al., 1994; Fransson and Israelsson, 1999). Moreover, the accuracy of the regression approach also depends on the number of points used in developing the regression curve which in turn translates into more accurate field measurements, a difficult process to be avoided.

Another problem with this approach, which results from the foregoing paragraph, is that the biomass values used in regression may not be quite accurate. Moreover, radar backscatter is a strong function of canopy moisture content, i.e., it is not merely the amount of woody biomass, but also the moisture contained in it that contributes to SAR measurements (Saatchi and Moghaddam, 1994). The same forest stand produces very different backscatter depending on whether it is experiencing drought, flood conditions, freezing, or thawing. Therefore, a valid biomass estimation algorithm must be

accompanied by some knowledge of environmental condition and moisture condition of stands. In this paper, such an algorithm is developed and demonstrated. First, we present a semi-empirical forest model derived from a more complicated physically based model. In this model, the biometric and structural parameters of forest canopy components are separated. Structural parameters are those related to the geometry and distribution of forest canopy components such as branches, leaves, and stems. These parameters can be determined by training the model once over known forest stands in a radar image. The biometric parameters such as crown and stem water content and carbon content (biomass) can be estimated from the model after the structural parameters are determined for forest types. The paper follows by discussing the BOREAS experiment, the general characteristics of the study area, biometry measurements of forest stands, and airborne imaging radar data acquired during the experiment in Section 2. Section 3 briefly describes the semi-empirical model and the characteristics of an algorithm for estimating crown and stem water content and biomass. Section 4 discusses the application and accuracy of the algorithm and the derived biomass maps over the BOREAS study area.

# II. BOREAS Experiment

## A. Study Area

The Boreal Ecosystem Atmospheric Study (BOREAS) is an international scientific effort to understand the interactions of the boreal landscape with the atmosphere. The experiment was designed: 1) to improve our understanding of the processes which govern the exchanges of energy, water, heat, carbon, and other trace gases, and 2) to develop and validate remote sensing algorithms for estimating parameters required to understand the above processes at different scales. The field and remote sensing measurements during the experiment were concentrated at two sites in Canada: the southern study area (SSA) is approximately 40 km north of Prince Albert, Saskatchewan and covers an area about 130 km in the east-west direction and 90 km from north to south (53.2°N, 105.7°W)(see Figure 2). The topography is gentle and varies about 200 m with local elevations ranging from 550 m to 730 m. The northern study area (NSA) is located roughly 500 km to the northwest near Thompson, Manitoba (55.7°N, 97.8°W). During the intensive field campaigns, forest canopy parameters such as biomass, canopy composition, and structural parameters were collected in both study areas. In this paper, we concentrate on the southern study area. The SSA is near the southern limit of the boreal forest and the transition to

natural prairie grasslands and agricultural fields. The age of Forest stands in this region range between 50 and 100 years. Tree heights in mature stands range from 15 to 22 m, although there are stunted black spruce in bog areas. The vegetation cover is predominantly coniferous and classified as mixed boreal forest. On well drained and/or sandy soil the predominant species is jack pine (*Pinus banksiana*). Poorly drained sites support black spruce (*Picea mariana*) that are often covered with thick layers of sphagnum and feather moss. Mixed stands of trembling aspen (*Populus tremuloides*), balsam poplar (*Populus balsamifera*), and white spruce (*Picea gluaca*) are found on well drained glacial deposits.

## B. Field Measurements

During the summers of 1993 and 1994, several BOREAS teams conducted inventory measurements of forest stands within the study area. These measurements included identification of tree species, density, DBH (measured at 1.37 m height), height, and age within sampling plots. The measurement data used in this study were collected by TE-6 (Terrestrial Ecology team # 6) in tower and auxiliary sites (Gower et al., 1997; Sellers et al., 1995). From the plot measurements and destructive sampling in August 1994, allometric regression equations were developed for three dominant overstory species: jack pine, black spruce, and trembling aspen. Often, separate sets of equations were developed for small and large trees depending on the DBH values. Using these site-specific allometric equations biomass, sapwood volume, and leaf area were estimated for each stand. The allometric equations for trembling aspen were for other deciduous trees such as balsam poplar. The biomass estimates included the tree components (main stem, branches, and foliage) on a per tree basis for each live stem. Biomass values for each tree were summed over each plot (four plots per stand) and expressed in terms of kilograms of carbon per hectare (kg carbon/ha). These values were then converted to crown and stem dry biomass in terms of $kg/m^2$. The four plots at each tower site varied from site to site based on number of stems per hectare; whereas, the auxiliary site plots were determined based on four prism points or fixed plots spaced 10 meters in the cardinal directions (Gower et al., 1996). Biomass values for plots were used to compute average and standard deviation of the stand crown and stem biomass. The results of biomass inventory of 18 stands within the area imaged by AIRSAR are summarized in Table 1.

In the process of developing allometric equations from the destructive sampling, moisture contents of tree components for dominant species were also recorded. For all trees, three sections, top, middle, and bottom were sampled for measuring the moisture

content of foliage, branches, and twigs (see Table 2). The dominant species used in moisture content measurements are jack pine, black spruce, trembling aspen, and young jack pine (8-12 years). For stems, the moisture contents were measured based on 2-meter sections and for each section the samples were taken from the lower end (Table 3). The quantities given in Tables 2 and 3 are simply the ratio of fresh weight minus dry weight over fresh weight. Note that the moisture content of stems for conifers increases with the stem height, whereas for deciduous trees remains approximately constant. To demonstrate this point, we have plotted the moisture contents of trees sections with respect to the tree heights in Figure 3.

## C. AIRSAR Data

The JPL airborne synthetic aperture radar (AIRSAR) was flown aboard the NASA DC-8 during all the intensive field campaigns (IFC) in summer of 1993, April 1994 during the thaw period of the boreal forest, and in summer and fall of 1994. The AIRSAR operates at three frequency bands, P-band (68 cm wavelength), L-band (24 cm), and C-band (5.6 cm) with fully polarimetric capability. The incidence angle of the radar varied between approximately $20^{o}$ and $60^{o}$. The radar data used for land-cover classification were acquired in July 21, 1994 and processed in synoptic mode (50 km swath). We have chosen this date to avoid possible errors in classification due to the partially frozen condition during the thaw period and leaf-off condition during the fall season. We have used images from several parallel flight lines in a mosaic mode to create larger area coverage over the modeling grid. The calibration, radiometric correction, and mosaic of the images were performed in several steps as follows:

## D. Image Calibration

In this study we have made use of synoptic SAR images which were acquired with parallel flight lines in a "race-track" mode. The synoptic images have larger coverage (approximately 50 km) but only three polarizations. These images are often processed for the purpose of surveying the area and are not absolutely calibrated. We have processed a total of 15 synoptic images to cover all the bands and polarizations of the AIRSAR system. Calibration of images are performed by using fully polarimetric calibrated frame images processed over a portion of the synoptic images. Absolute calibration constants were obtained by computing the ratios of backscattering coefficients from identical areas from both images and applying the calibration constants to all synoptic images. When compared with frame images, the synoptic images were absolutely calibrated with less than 0.1 dB error for all polarization channels. The frame images were calibrated both internally and

externally using data collected over an array of corner reflectors deployed over the Rosemond dry lake calibration site in California before and after the AIRSAR campaign. After the absolute calibration, the images were resampled to ground range to remove the distortions in the near range and far range pixels.

## E. Incidence Angle Correction

One of the disadvantages of airborne SAR data, when used for land-cover classification, is the variation of the incidence angle along the range lines across the image ($20^{o}$-$60^{o}$). Consequently, areas with similar land-cover types produce different backscatter signatures if they are imaged at different incidence angles and depending on the scene characteristics, the variation of the backscatter signature along each range line may be different. These effects can cause inaccuracies in a consistent class separation over the entire image. Correction of the image for incidence angle effects, therefore, becomes a necessary but impossible task to accomplish exactly.

The synoptic images used in this study were corrected for incidence angle variations according to Saatchi and Rignot (1996). This approach was discussed in detail and compared with other approaches in the literature. We plotted the incidence angle variations for each range line, then a nonlinear regression in conjunction with a cubic spline smoothing algorithm was used to estimate the general behavior of the incidence angle variations along each range line. The regression curve was then normalized by the mean backscattering coefficient of the range line and then used to correct for the incidence angle effects of that range line. The entire image was then corrected line by line. As a result of this correction, the near range (small incidence angles) and far range (large incidence angles) backscatter values are transformed such that they represents the mid-range incidence angles (about $35^{o}$-$45^{o}$).

## F. Image Mosaic

After calibration and incidence angle correction, the images from each frequency band and polarization were used in tandem to generate a mosaic image over almost the entire modeling sub-grid. Figure 4 shows a color composite of the mosaic image at P-band (red: P-HH, green: P-HV, blue: P-VV). Since the images were acquired from flight lines with the same heading, they also had an area of overlap with adjacent images. A linear feathering technique was then employed to remove the tonal inconsistencies that existed at the areas of overlap. In some areas where incidence angle effects were not optimally

corrected, the feathering technique guaranteed further smoothing at the edges of images. If the overlapping regions were near the lakes where there was a dramatic change in the radar backscatter signature, incidence angle effects could not be totally removed and the edge effects were still obvious in the mosaic image. The final mosaic image was then georeferenced and co-registered with land cover maps available in BOREAS information system (Saatchi and Rignot, 1997). Note that in the process of removing the incidence angle variations, image mosaicking, and co-registeration, the absolute values of SAR backscattering coefficients and its variability and dynamic range over the scene were preserved. However, the absolute value of incidence angle for each pixel has been altered. The incidence angle variations over the entire mosaic image is between 40° and 50°.

# III. Algorithm

The radar backscatter from vegetated surfaces is controlled by two sets of parameters: 1) geometric parameters related to the structure of vegetation and soil, and 2) dielectric parameters related to the moisture content of plants and underlying soil surface. Environmental and physiological conditions, such as availability of water, freezing condition, and leaf out and senescence influence the structural and moisture parameters. The sensitivity of microwave backscatter data to the above ground woody biomass is primarily due to structure and moisture dependent information in the data. Recent studies are primarily focused on developing regression type algorithms for directly estimating vegetation biomass from radar data (Dobson et al., 1995; Ranson and Sun, 1994; Ranson et al., 1995, 1997, Rignot et al., 1994). However, since both structure and moisture parameters exert control over polarization, frequency band, and angular dependence of radar backscatter data, these algorithms become site specific and will not perform well under different environmental conditions (Dobson et al., 1995).

In this study, we use an alternative approach, by first estimating the forest canopy moisture content and then using conversion factors between dry and wet weight to estimate the above ground woody biomass. The estimation of canopy water content is performed by using a semi-empirical model for boreal type forests developed by Saatchi and Moghaddam (1999). The model is based on analytical simplifications of a two layer forest backscatter model in order to separate structural and dielectric parameters in forest crown and stem layers. This model has been discussed in detail elsewhere (Saatchi and McDonald 1997). The determination of structural parameters for various forest types will provide a simple model for estimating crown and stem water content and biomass.

It is assumed that over forest canopies, the total backscattering coefficients consist of three dominant scattering mechanisms: crown volume scattering, crown-ground scattering, and trunk-ground scattering. Figure 4 illustrates the first order (no multiple scattering) dominant scattering contributions. The expressions for each contribution includes scattering cross sections of canopy constituents (leaf, branch, stem) that includes parameters related to size and angle distributions, and dielectric constants (Saatchi and McDonald, 1997; Lang et al., 1994). These expressions are mathematically complicated and are not generally suited for model inversion. The major obstacle is the mixing of dielectric and structural parameters in scattering and absorption terms in the model. The approximations introduced by Saatchi and Moghaddam (1999) allows these two sets of parameters to be separated in the expressions defining the backscattering coefficients. While the general form of the mathematical expressions are preserved, the simple form suggests the structural parameters can be estimated using data from model simulations or by training the model with the SAR backscatter measurements over known forest stands. As a result, a simple semi-empirical model is developed that include only moisture parameters of vegetation and soil surface for a certain forest type. In what follows, we present the general form of the simplified model and refer the interested reader to Saatchi and Moghaddam (1999) for more detailed discussion. However, since the model has preserved in its general form and we discuss all the terms and parameters in detail, the reader is not require to consult other sources for understanding the characteristics of the model.

In general, the total backscattering coefficient measured by SAR is given by:

$$\sigma^0_{pq} = \sigma^0_{pqc} + \sigma^0_{pqcg} + \sigma^0_{pqtg} \qquad (1)$$

where p and q represent the electromagnetic wave polarizations of the received and transmitted radar signals, and c, cg, and tg represent the crown, crown-ground, and trunk-ground scattering mechanisms respectively. In the above expression, we have assumed that the forest canopy consists of two layers (crown and trunk) and the direct contribution from the soil surface is small compared to other scattering mechanisms. The simplified expressions for the scattering mechanisms are given as follows:

$$\sigma^0_{pqc} = k_0 \frac{|\varepsilon_w|^{1.3}}{\varepsilon''_w} \cos\theta_i \gamma_{pqc} W_c \left(1 - e^{-k_0 \varepsilon''^{0.65}_w \sec\theta_i \beta_{pqc} W_c}\right) \qquad (2)$$

$$\sigma^0_{ppcg} = k_0^{1.4} |\varepsilon_w|^{1.3} e^{-k_0^2 s^2 \cos^2\theta_i} \Gamma_p \gamma_{ppcg} W_c e^{-k_0 \varepsilon''_w \sec\theta_i (\beta_{ppc} W_c + \beta_{ppt} W_t)} \qquad (3)$$

$$\sigma^0_{pptg} = k_0 \sin\theta_i \left|\varepsilon_w\right|^{0.65} e^{-k_0^2 s^2 \cos^2\theta_i} \Gamma_p \gamma_{pptg} W_t e^{-k_0 \varepsilon''_w \sec\theta_i (\beta_{ppc} W_c + \beta_{ppt} W_t)} \quad (4)$$

where

$k_0$ = wavenumber

$\theta_i$ = incidence angle

$\varepsilon_w = \varepsilon'_w - i\varepsilon''_w$ = dielectric constant of water

$s$ = *rms* height of surface roughness

$\Gamma_p$ = Fresnel reflectivity of surface at polarization $p \in \{h, v\}$

$W_c$ = crown moisture content

$W_t$ = trunk (stem) moisture content.

The Fresnel reflectivity of soil surface depends on the relative dielectric constant of soil, $\varepsilon_g$ which is assumed to be real for simplicity. The remaining parameters, $\beta_{hht}$, $\beta_{vvt}$, $\gamma_{hhtg}$, $\gamma_{vvtg}$, $\beta_{hhc}$, $\beta_{vvc}$, $\gamma_{hhc}$, $\gamma_{hvc}$, $\gamma_{vvc}$, $\gamma_{hhcg}$, $\gamma_{vvcg}$, in equations (2)-(4) represent the average attenuation and scattering cross sections for the ensemble of scatterers within a forest canopy are solely dependent on the geometrical attributes of the forest canopy and are approximately independent of frequency and moisture content. The dielectric constants of water are given from mixing models at various frequencies and are listed below (Ulaby et al, 1986).

$$\begin{aligned} \varepsilon_w &= 72.0 - i28.4 \quad \text{C - band (5.3 GHz)} \\ \varepsilon_w &= 83.2 - i7.81 \quad \text{L - band (1.25 GHz)} \\ \varepsilon_w &= 83.9 - i2.77 \quad \text{P - band (0.44 GHz)} \end{aligned} \quad (5)$$

In deriving the above relations, we have assumed that the tree trunks are vertically distributed and their scattering contribution is in trunk-ground interaction term (commonly known as double-bounce term) and in co-polarized channels (Saatchi and McDonald, 1997; Lang et al., 1994). The crown-ground scattering term is also important in the co-polarized backscattering and does not have a significant cross-polarized contribution (Moghaddam and Saatchi, 1995; Saatchi and McDonald, 1997). In most cases, the crown-ground scattering is smaller than the truck-ground scattering. Model simulations have shown that the crown-ground contribution is only due to branches whose lengths are much longer than wavelength and are distributed in vertical direction like trunks, while small branches and

leaves contribute primarily in the direct backscattering term. The scattering from the crown layer contributes in all polarization channels and is also the main source of attenuation in radar channels. Although these assumptions are based on model simulations for specific forest types, they are shown to explain the characteristics of the SAR data over forest canopies (Moghaddam and Saatchi, 1995; Richards et al., 1987; Sun et al., 1991). The errors from these assumptions and the general performance of the model have been discussed in our earlier works (Saatchi and McDonald, 1997; Moghaddam and Saatchi, 1995; Saatchi and Moghaddam, 1999).

Given the underlying rationale for model expressions, the structural parameters can be estimated from the original model simulations if the geometrical information of the forest canopy such as size, angle, and spatial distributions of leaves, branches, and stems are known. In most cases, to obtain such information requires detailed destructive sampling of the forest canopy. This process is extremely time consuming and the obtained information are often not representative of variabilities that occur in nature. The alternative approach would be to estimate the structural parameters directly from the backscatter data over forest stands whose crown and stem biomass and soil surface characteristics are known. This procedure will transform the model to a semi-empirical model whose unknown coefficients are obtained from the SAR data and therefore adjusted to the calibration of the backscatter measurements at all channels.

In addition to the above assumptions for model simplifications, we have also assumed that the crown and stem biomass are independent variables in the model. In general, there can be a relationship between crown and stem biomass. However, as it is shown in figure 5 for 65 sites in the BOREAS study area, this relationship is not well defined and can vary with forest type and structure and may be influenced by environmental conditions and soil moisture availability (Bonan et al., 1990; Botkin, 1993).

The knowledge of structural parameters in equations (2)-(4) will allow the model to depend only on instrument parameters such as polarization, wavelength and look angle, and forest biometric parameters. Among the structural parameters, those associated with stem scattering, $\beta_{hht}$, $\beta_{vvt}$, $\gamma_{hhtg}$, $\gamma_{vvtg}$ are estimated from the original model simulations because the orientation of stems are assumed vertical. The estimation of the remaining parameters, $\beta_{hhc}$, $\beta_{vvc}$, $\gamma_{hhc}$, $\gamma_{hvc}$, $\gamma_{vvc}$, $\gamma_{hhcg}$, $\gamma_{vvcg}$ requires at least seven independent measurements that can be readily provided by polarization and frequency diversity of AIRSAR radar system.

It is important to mention that the required measurements must be sensitive to desired parameters. For example, to estimate the crown and stem water content and

biomass, it is known that measurements at lower frequencies such as L-band and P-band are more appropriate (Ranson et al., 1995; Dobson et al., 1992; Le Toan et al, 1992). In estimating these parameters from regression analysis, one needs to establish a relationship between each channel of radar data and the desired parameter separately (Dobson et al., 1995). However, since the model shown in equations (2)-(4) is a physically based representation of the backscattering, it automatically weighs the contribution of each scattering mechanism for all frequency and polarization channels of radar data.

# IV. Estimation of structural parameters

Having developed a simplified radar backscatter model for forest canopies, we use JPL AIRSAR data and biometry field measurements of crown and stem water content over homogeneous stands for each forest type to estimate the structural parameters in equations (2)-(4). Field measurements provide data for forest and soil characteristics of trembling aspen (TA), old jack pine (OJP), old black spruce (OBS), and young jack pine (YJP). The JPL AIRSAR data are synthesized into three polarizations (HH, HV, VV) for each of the three bands (P-, L-, C-bands) to provide nine images. In addition, during the AIRSAR overflight, surface soil moisture and rms height were measured at each site. After using the biometric data in model equations for each stand, the Levenberg-Marquardt nonlinear least-squares method was used to estimate the structural parameters (Press et al., 1990). Radar backscatter data from AIRSAR images were extracted on pixel-by-pixel basis in a polygon over each stand in order to generate a statistically significant sample population for mean and variance of backscattering coefficients over each stand.

The backscattering coefficients from nine AIRSAR channels were used as input data in the estimation procedure. The estimation of structural parameters was then performed by an iterative method in order to optimized the least square error (less than 1 dB) between SAR measurements and semi-empirical model results. Initial values for each parameter in the iterative procedure were provided by the original model simulations using the stand parameters. The parameters estimated for each stand are given in Table 4. Note that these parameters are obtained assuming that the forest stands are homogeneous such that mixed species and forest gap information have not been accounted for in the model. In the case of mixed stands and in the presence of large gaps in the forest canopy, we predict that these parameters will be less accurate. Nevertheless, since the image data over the stand and biometric data from field measurements are incorporated in the estimation process, we believe that retrieved structural parameters are somehow representative of

density and species variations within the stands. However, at this stage we do not enough data to investigate the errors associated with canopy inhomogeneities.

Because the contributions of the three scattering mechansims, crown, crown-ground, and trunk-ground for each radar channel may vary, the semi-empirical estimation algorithms automatically weighs different scattering contributions depending on the forest type. For example, for old jack pine stands, the main contribution in C-band channels is due to volume scattering of crown layer, whereas at L-band and P-band both the crown-ground and trunk-ground interaction terms are also significant. Since all these terms with their proportional coefficients (depending on frequency) are incorporated in the model, the procedure estimates the parameters automatically and all at the same time in order to satisfy the error criteria (Press et al., 1990).

By removing the forest type in the estimation process, we will find mean structural parameters that can apply to any forest type in the boreal region. Of course, the accuracy of the resulting equations will suffer from the generic structural parameters. In situations where the forest land cover types are not known, these parameters can be estimated by choosing a large polygon over the image data as the training area. It is important to mention that for each forest type, the structural parameters are obtained only once and the derived semi-empirical algorithm can be used for any radar backscatter data assuming the radar measurements are cross calibrated.

Table 4 shows the structural parameters estimated for four dominant forest types, old jack pine, young jack pine, black spruce, and trembling aspen, in the study area. As mentioned earlier, out of the eleven structural parameters, the four related to the stem distributions are obtained from the original model simulations. For each forest types, we have extracted the pixel-by-pixel extraction of SAR data from all the channels. The number of pixels for each forest types are indicated in the table.

Using the structural parameters in equations (2)-(4), we readily obtain backscattering equations which are specific to forest types and consist of four unknown parameters, $W_c$, $W_t$, s, $\varepsilon_g$. A total of nine equations are obtained for the three frequency and three independent polarizations (CHH, CHV, CVV, LHH, LHV, LVV, PHH, PHV, PVV) of the AIRSAR system. After the estimation of structural parameters, we demonstrated the accuracy of the simplified model by comparing its simulations over a known stand with the original model. The simulations were performed for a jack pine stand with known geometric and biometric characteristics and by varying the forest crown and stem biomass, soil moisture and roughness parameters. The forest attributes used in the simulations are given in Saatchi and McDonald (1997). A total of 625 simulation data, obtained by choosing 5 values for each parameter. The difference between the semi-

empirical model and the original model for the jack pine stand stayed less than 5% at all times, suggesting the acceptable performance of the semi-empirical model.

To estimate the four unknown parameters, we require four independent radar measurements over the forest canopy that are at the same time sensitive to these parameters. For example, measurements at P- and L-band are more suitable for estimating the stem parameters than at C-band. The sensitivity of each band and polarization combination has been discussed elsewhere (Rignot et al., 1994; Moghaddam et al., 1995). However, as in the case of the structural parameters, we use all the available channels in order to gain better accuracy in estimating the desired parameters. Note that since the equations have the proper weights for frequency and polarization characteristics of SAR data, the use of more channels (instead of four) does not reduce the accuracy of estimation. In this paper, we are primarily concerned with forest water content and biomass parameters. Therefore, we will not discuss the issues pertaining to the estimation of soil surface parameters, even though the algorithm automatically estimates all four parameters at the same time by using a nonlinear estimation technique as discussed earlier.

# V. Results and Discussion

## A. Validation of Algorithm Over Test Sites

To validate the algorithm, we use the SAR data extracted from the tower and auxiliary sites where the forest stands are homogeneous and are dominated primarily by one species. The backscattering coefficients extracted from a polygon over the sites are then used in a nonlinear least square inversion (Levenberg-Marquardt) approach to estimate the crown and stem water content. Table 5 shows the results and the errors as compared with the data obtained from ground measurements reported by the BOREAS science teams. The measured crown and stem dry biomass are derived from applying the ratio of water content to dry biomass given in Tables 2 and 3. The estimated values in Table 5 are obtained by computing the mean and standard deviation of biomass for the same polygons. For stands that contain mixed species, the water content is calculated by adjusting the water content ratios from the species composition information given by the SAR classification results reported in Saatchi and Rignot (1997).

The overall least-square estimation error of all 18 sites stays below 10%. However, the difference errors for individual sites may be larger. In estimating the canopy water content, we have used all nine channels of radar data. However, since there are only four unknowns to be estimated, it is possible to select four most sensitive radar channels for the parameter retrieval. The estimation errors are not entirely due to the performance of the algorithm and are also caused by the uncertainties of the field data collected during the experiment. These uncertainties are primarily due to the natural inhomogeneities of forest ecosystem and inaccuracies associated with the use of empirical allometric equations to estimate forest biomass. The uncertainties in ground measurements are shown in Figure 1 and are numerically presented in Table 1. The errors in *in situ* biomass measurements increase with biomass and can vary by more than 100 tons/hectare for mature and mixed stands.

The algorithm for water content and biomass estimation appear to be the same. Once the water content is obtained a proportionality coefficient (the ratio of dry to wet biomass) can readily provide the biomass. It is therefore possible to include these coefficients in the formulation of the algorithm for each stand in order to derive a direct biomass estimation algorithm. The resulting biomass algorithm will be inherently different from regression type algorithms (Ranson and Sun, 1994; Dobson et al., 1997) because both the structural and canopy moisture information are present in the model formulation.

## B. Biomass Mapping

As it was discussed earlier, the biomass estimation over individual stands is carried out by applying the average ratio of the dry weight to water content to the crown and stem water content estimation of each forest type. By applying these ratios, we ignore the moisture variations within each tree type as shown in table 2 and 3 and figure 3. However since the tree level moisture variation is smaller than the spatial variability of biomass of each forest stand (Figure 1), by including the variations of moisture in computing the above ground dry biomass, we do not gain a significant improvement in biomass estimation.

To apply the algorithm to the image data for pixel-by-pixel estimation of biomass, we used the land cover map derived from the SAR data (Saatchi and Rignot, 1997). The map separates eight forest types from which three are the dominant species of jack pine, black spruce and aspen, and the rest are mixed forest classes, open water and nonforest areas. For mixed forest types, we computed new structural parameters similar to single species stands. In the absence of a land cover map, the algorithm can be applied to the

entire image by using average structural parameters estimated by training the model over the entire image by excluding water and land use pixels. Of course, in this case the accuracy of the biomass estimation reduces.

To demonstrate the performance of existing or future spaceborne SAR systems in estimating the boreal forest biomass, we estimated the biomass over the BOREAS sites using several combinations of AIRSAR channels. In table 6, we provide biomass estimation errors for various combination of radar channels. The best estimates are obtained by choosing the combination of PHH, PHV, LHV, and CHV. The cross-polarized channels at C- and L-band are primarily due to crown scattering mechanism and therefore are more sensitive to crown water content and biomass. At P-band the radar signal penetrates through the entire canopy and is more sensitive to the stem water content. In particular, the co-polarized channels such as PHH are primarily due to trunk-ground interaction scattering attenuated by the crown layer. In order to avoid the ill-posed problem of having fewer measurements than unknowns in the estimation procedure, we have set the soil moisture (dielectric constant )to measured values obtained during the field experiment at the time of SAR overflights. These measurements are performed over tower sites but used for auxiliary sites as well. The reason for choosing soil moisture as a known parameter in the algorithm instead of soil surface roughness, is mainly due to the higher sensitivity of radar backscatter to soil roughness of forest floor and the fact that it is a difficult parameter to measure.

The estimation accuracy for L-band and P-band polarimetric data are similar. This is primarily due to the fact that the above ground biomass in the boreal forests are often less than the saturation limit of backscatter at these frequencies. However, we expect that the performance of P-band data for biomass estimation over other ecosystems such as temperate and tropical forests would be better than L-band.

# 5. Summary and Conclusion

In this paper, the crown and stem water content and biomass of boreal type forests have been estimated from multifrequency and multipolarization SAR data. A new algorithm based on a semi-empirical and physically based model is used to estimate the forest parameters. The model has two main features: 1) the structural parameters that define the distribution and shape of leaves, branches, and stems are separated from biometric parameters such as water content and dry biomass, and 2) a land cover map is required to allow the training of the model for structural parameters, and the accurate estimation of the biometrics parameters. Unlike other regression type models, these

features allow the model to be used for any forest type and radar data with a minimum number of sites for developing the retrieval algorithm. In the example discussed in this paper, for each forest type, we used only one training site. Moreover, by using an average structural parameter, the algorithm can be employed without the use of a land cover map. The only disadvantage of this model in comparison with the regression models is the fact that the model has to be trained for the estimation of the structural parameters.

The algorithm was used to estimate crown and stem biomass from AIRSAR mosaic image over the BOREAS southern study area. The result of the estimation showed that the L-band and P-band polarimetric data had similar accuracy in retrieving the biomass components. The highest accuracy (more than 90%) was achieved when all radar channels were used in the estimation procedure. The biomass variance obtained from the algorithm over the test sites was much smaller than the ones obtained from the field data and shown in figure 1 and Table 5. These results indicated that once a reliable algorithm was developed for biomass estimation from remote sensing data, its performance could be superior to the traditional forestry methods. However, this needs to be proved and verified over several forest sands with a variety of environmental conditions.

We also used the algorithm, with some assumptions about the soil moisture and roughness, with different combination of radar channels in order to simulate scenarios for the use of spaceborne radar. A combination of JERS-1 LHH, ERS-1 CVV, and RADARSAT CHH channels showed only 60% accuracy. Future systems such as L-band polarimetric radar (lighter) showed 80% accuracy. As the average biomass of the circumpolar boreal belt is less than 100 tons/ha, we expect to be able to map the entire boreal forest biomass from an L-band polarimetric system such as lighter. Furthermore, given the fact that the images acquired by spaceborne systems have small incidence angle variations and a better relative and absolute calibration, the structural parameters can be derived a priori for various forest types and used as a lookup table for generating a biomass map.

# Acknowledgment

This work was performed at the Jet Propulsion Laboratory, California Institute of Technology, under contract with the National Aeronautics and Space Administration.

# References


Bonan, GB, and H.H. Shugart, and D.L. Urban, "The sensitivity of some high-latitude boreal forests to climate parameters", *Climate Change*, 16, 9-29, 1990.

Botkin, D.B., *Forest Dynamics: An Ecological Model*, Oxford University Press, New York, NY, 1993.

The Boreas Information System (http://boreas.gsfc.nasa.gov/), 1996.

Brown S., and A.E. Lugo,"Tropical secondary forests", J. Tropical Ecology, 6:1-32, 1990.

Davis, M.B., and D.B. Botkin, Sensitivity of cold temperate forests and their fossil pollen to rapid climate change, *Quat. Res.*, 23, 327-340, 1985.

Dobson, M.C., F.T. Ulaby, T. LeToan, A. Beaudoin, E.S. Kasischke, and N. Christensen, Dependence of radar backscatter on conifer forest biomass, *IEEE Trans. Geosci. Remote Sens.*, GE-30, 412-415, 1992.

Dobson, M.C., F.T. Ulaby, L.E. Pierce, T.L. Sharik, K.M. Bergen, J. Kellndorfer, J.R. Kendra, E. Li, Y.C. Lin, A. Nashashibi, K. Sarabandi, Estimation of forest biophysical characteristics in Northern Michigan with SIR-C/X-SAR, *IEEE Trans. Geosci. Remote Sens.*, GE-33, 877-895, 1995.

Fransson, J.E.S., and H. Israelsson, "Estimation of setm volume in boreal forests using ERS-1 C- and JERS-1 L-band SAR data," *Int. J. Remote Sensing*, vol. 20, 123-137, 1999.

Gower, S.T., J.G. Vogel, J.M. Norman, C.J. Kucarik, S.J. Steele, and T.K. Stow, "Carbon distribution and above ground net primary production in aspen, jack pine, and black spruce stands in Saskatchewan and Manitoba, Canada," *J. Geophysical Research*, vol. 102, No. D24, 29029-29041, 1997.

Hussin, Y.A., R.M. Reich, and R.M. Hoffer, "Estimating slash pine biomass using radar backscatter," *IEEE Trans. Geosci. Remote Sensing*, vol. 29, 427-431, 1991.

Keeling, C.D., J.F.S. Chin, and T.P. Whorf, "Increased activity of northern vegetation inferred from atmosphere Co2 measurements," Nature, 382:146-149, 1996.

Kimball, J, S. Saatchi, and S. Running, Sensitivity of boreal forest regional water flux and net primary production simulations to sub-grid scale land cover complexity, *J. geophysical Research*, BOREAS II Special Issue, In Press, 1999.

Lang, R.H., N.S. Chauhan, K.J. Ranson, and O. Kilic, Modeling P-band SAR returns from a red pine stand, *Remote Sens. Environ.* 47, 132-141, 1994.

Le Toan, T., A. Beaudoin, J. Riom, and D. Guyon, "relating forest biomass to SAR data," *IEEE Trans. Geosci. Remote Sensing* vol. 30, pp. 403-411, 1992.

Moghaddam, M., S. Durden, and H. Zebker, "Radar measurement of forested areas during OTTER," *Remote Sens. Environ.,* vol. 47, 154-166, 1994.

M. Moghaddam and S. Saatchi,"Analysis of scattering mechanisms in SAR imagery over boreal forest: Results from BOREAS'93," *IEEE Trans. Geosci. Remote Sensing*, GE-33, 1290-1296, 1995.

Ranson, K.J., and G. Sun, Mapping biomass for a northern forest using multifrequency SAR data, *IEEE Trans. Geosci. Remote Sens.*, GE-32, 388-396, 1994.

Ranson, K.J., S.S. Saatchi, and G. Sun, Boreal forest ecosystem characterization with SIR-C/X-SAR, *IEEE Trans. Geosci. Remote Sensing*, GE-33, 867-876, 1995.

Ranson, K.J., G. Sun, R. Lang, N. Cahhan, R. Cacciola, and O. Kilic, "Mapping of boal forest biomass from spaceborne synthetic aperture radar," *J. Geophysical Research,* vol. 102, No. D24, 29599-29610, 1997.

Rauste, Y., T. Hame, J. Pullianen, K. Heiska, and M. Hallikainen, "Radar-based forest biomass estimation," *Int. J. remote Sensing,* vol. 15, 2797-2808, 1994.

Richards, J.A., G. Sun, and D.S. Simonett, "L-band radar backscattering modeling of forest stands," *IEEE Trans. Geosci. Remote Sensing*, vol. 25, 487-498, 1987.

Rignot, E., J. Way, C. Williams, and L. Viereck, Radar estimates of above ground biomass in boreal forests of interior Alaska, *IEEE Trans. Geosci. Remote Sens.*, GE-32, 1117-1124, 1994.

Running S.W., and J.C. Coughlan, "A general model of forest ecosystem processes for regional applications I. Hydrological balance, canopy gas exchange and primary production," Ecological Modeling 42:125-154, 1988.

Saatchi, S., and M. Moghaddam, Biomass distribution in boreal forest using SAR imagery, in Multispectral and microwave sensing of forestry, hydrology, and natural resources, Ed. by E. Mougin, K.J. Ranson, and J. Smith, Proc. Europta Series, SPIE vol. 2314, September 26-30, 437-448, 1994.

Saatchi, S., J. van Zyl, G. Assrar, Estimation of canopy water content in Konza prairie grasslands using synthetic aperture radar measurements during FIFE, *J. Geophys. Res.* 100, D12, 25481-25496, 1995.

Saatchi, S., and K. McDonnald, "Coherent effects in microwave backscattering models for forest canopies," *IEEE Trans. Geosci. Remote Sensing*, Vol. 35, No. 3, 585-598, 1997.

Saatchi, S., and E. Rignot, " Land cover classification of BOREAS modeling grid using AIRSAR Images," *Remote Sens. of Environ*, Vol. 35, No. 6, 270-281, 1997.

Saatchi, S. and M. Moghaddam, " Retrieval of forest canopy parameters from polarimetric SAR data: I. theory," submitted to *IEEE Trans. Geosci. Remote Sensing, Feb., 1999.*

Sellers, P., et al., "The boreal ecosystem-atmosphere study (BOREAS): An overview and early results from the 1994 field year," Bull. Am. Met. Soc., 76:1549-1557, 1995.

Sun, G., D.S. Simmonet, and A. Strahler, "A radar backscatter model for discontinous coniferous forests," *IEEE Trans. Geosci. Remote Sensing,* vol. 29, 639-650, 1991.

Tans, P.P., I.Y. Fung, and T. Takahashi, Observational constratints on the global atmospheric $CO_2$ budget, *Science*, 247, 1431-1438, 1990.

Ulaby, F.T., R.K. Moore, A.K. Fung, *Microwave Remote Sensing: Active and Passive, Vol. III-Volume Scattering and Emission Theory*, Advance System and Applications series, Artech House, Dedham, Massachusetts, 1986.

# Figure Caption

Figure 1. Comparison of field biomass measurement of BOREAS sites. The measurements are performed over the same forest stands by two groups. The mean and standard deviations are calculated from biomass values over 3 plots for Forestry Canada data, and 4 plots for BOREAS data.

Figure 2. Map of BOREAS southern study area and the location of tower sites.

Figure 3. Variations of stem water content with respect to height for four dominant forest stands, TA (Trembling Aspen), OJP (Old Jack Pine), OBS (Old Black Spruce), YJP (Young Jack Pine) in the southern study area.

Figure 4. P-band polarimetric color overlay of the AIRSAR mosaic image of the modeling subgrid within the BOREAS southern study area acquired on 21 July 1994. P-band HH, HV, and VV polarizations are in red, green, and blue, respectively. The mosaic image is coregistered with the vegetation cover map and georeferenced to universal transverse Mercator coordinates with North being parallel to the side of the image.

Figure 5. Schematic diagram of dominant scattering mechanisms used in the semi-empirical model.

Figure 6. The relation between crown and stem biomass for three dominant forest stands in the BOREAS study areas. The figures are generated by using all available data points from the BOREAS information system including northern and southern study areas. The measurements are taken from TE6 field data.

Figure 7. Maps of forest crown and stem biomass derived from AIRSAR data. The caption shows the same color chart for crown and stem biomass with different number associated with colors.

Table 1. Crown and stem woody biomass estimates over selective tower and auxilary sites within SSA. The mean and standard deviation for each stand is computed from four plot samples.

| | Crown (tons/ha) | | Stem (tons/ha) | |
|---|---|---|---|---|
| Site ID | mean | std. | mean | std. |
| G2L7S | 8.15 | 6.07 | 20.29 | 13.64 |
| G9I4S | 35.88 | 14.83 | 97.92 | 29.60 |
| G2I4S | 42.89 | 8.41 | 108.28 | 28.9 |
| G6K8S | 19.73 | 3.69 | 61.18 | 6.15 |
| F1N0M | 33.36 | 4.94 | 142.43 | 35.40 |
| G8L6P | 5.16 | 2.24 | 7.42 | 5.31 |
| F5I6P | 7.72 | 1.06 | 68.16 | 12.41 |
| G9L0P | 20.97 | 5.52 | 94.42 | 20.69 |
| F7J0P | 45.17 | 18.79 | 165.60 | 33.52 |
| F7J1P | 31.25 | 1.51 | 151.28 | 120.21 |
| G4K8P | 26.52 | 6.85 | 94.54 | 23.04 |
| G1K8P | 23.97 | 8.87 | 98.08 | 40.07 |
| G7K8P | 15.57 | 4.94 | 65.09 | 20.86 |
| G4I3M | 44.31 | 2.45 | 131.36 | 70.86 |
| TE-OA | 18.32 | 5.69 | 158.92 | 31.09 |
| TE-OBS | 23.51 | 5.53 | 71.82 | 12.90 |
| TE-OPJ | 9.86 | 3.55 | 51.25 | 12.14 |
| TF-YJP | 8.87 | 2.88 | 15.22 | 4.91 |

Table 2. Water content of canopy components of dominant species of SSA. The quantities are the average of ratio of water content to fresh biomass and they are obtained from the bottom (BOT), middle (MID), and top (TOP) of several trees at tower sites. The species are trembling aspen (TA), old jack pine (OJP), old black spruce (OBS), young jack pine (YJP).

| | **Foliage** | | | **Twig** | | | **Branch** | | |
|---|---|---|---|---|---|---|---|---|---|
| Forest Type | BOT | MID | TOP | BOT | MID | TOP | BOT | MID | TOP |
| **TA** | 0.663 | 0.666 | 0.654 | ------ | ------ | ------ | 0.480 | 0.437 | 0.472 |
| **OJP** | 0.369 | 0.316 | 0.553 | 0.375 | 0.364 | 0.415 | 0.364 | 0.353 | 0.418 |
| **OBS** | 0.452 | 0.416 | 0.404 | 0.369 | 0.353 | 0.331 | 0.316 | 0.307 | 0.324 |
| **YJP** | 0.369 | 0.316 | 0.366 | 0.375 | 0.364 | 0.415 | 0.364 | 0.353 | 0.418 |

Table 3. Stem water content of dominant forest types of SSA measured at 2 meter height interval.

| Forest Type | 2-4 | 4-6 | 6-8 | 8-10 | 10-12 | 12-14 | 14-16 | 16-18 | 18-20 | 20-22 |
|---|---|---|---|---|---|---|---|---|---|---|
| **TA** | 0.402 | 0.419 | 0.418 | 0.420 | 0.408 | 0.408 | 0.403 | 0.421 | 0.440 | 0.464 |
| **OJP** | 0.399 | 0.423 | 0.445 | 0.495 | 0.543 | 0.568 | | | | |
| **OBS** | 0.410 | 0.435 | 0.446 | 0.451 | 0.493 | 0.577 | | | | |
| **YJP** | 0.556 | 0.575 | 0.603 | | | | | | | |

Table 4. The structural parameters of forest types estimated from model simulations and SAR data. Among the structural parameters those related to stem are estimated from model simulations. Crown and stem biomass, soil moisture, and surface roughness for each forest stands are obatined from field measurements.

| Forest Parameters | TA | OJP | OBS | YJP |
|---|---|---|---|---|
| $W_c$ (kg/m$^2$) | 1.832 | 0.986 | 2.351 | 0.887 |
| $W_t$ (kg/m$^2$) | 15.89 | 5.251 | 7.182 | 1.522 |
| s (cm) | 1.3 | 0.89 | 3.2 | 1.8 |
| sm (percent) | 21% | 10% | 14% | 12% |
| $\beta_{hhc}$ | 0.00075 | 0.00035 | 0.00015 | 0.00063 |
| $\beta_{vvc}$ | 0.00091 | 0.00042 | 0.0091 | 0.00076 |
| $\beta_{hht}$ | 0.00150 | 0.00150 | 0.0015 | 0.00150 |
| $\beta_{vvt}$ | 0.00290 | 0.00290 | 0.00290 | 0.00290 |
| $\gamma_{hhc}$ | 0.00021 | 0.00048 | 0.00018 | 0.00017 |
| $\gamma_{hvc}$ | 0.00005 | 0.00011 | 0.00006 | 0.00008 |
| $\gamma_{vvc}$ | 0.00022 | 0.00025 | 0.00010 | 0.00012 |
| $\gamma_{hhcg}$ | 0.00017 | 0.00023 | 0.00017 | 0.00013 |
| $\gamma_{vvcg}$ | 0.00031 | 0.00041 | 0.00031 | 0.00023 |
| $\gamma_{hhtg}$ | 0.00303 | 0.01205 | 0.00170 | 0.000005 |
| $\gamma_{vvtg}$ | 0.01102 | 0.03019 | 0.01691 | 0.01005 |

Table 5. Comparison of estimated and measured crown and stem biomass. The error % in the table reference to the difference error between the estimated and measured quantity and the *rms* error % is the total estimation error.

| | Crown (tons/ha) | | | Stem (tons/ha) | | |
|---|---|---|---|---|---|---|
| Site ID | meaured | estimated | error % | measured | estimated | error % |
| G2L7S | 8.15 | 6.07 | 25.52 | 20.29 | 23.64 | 16.51 |
| G9I4S | 35.88 | 34.83 | 2.92 | 97.92 | 92.60 | 5.43 |
| G2I4S | 42.89 | 28.41 | 33.76 | 108.28 | 128.9 | 19.04 |
| G6K8S | 19.73 | 16.69 | 15.40 | 61.18 | 60.15 | 1.66 |
| F1N0M | 33.36 | 34.94 | 4.73 | 142.43 | 135.40 | 4.93 |
| G8L6P | 5.16 | 4.24 | 17.83 | 7.42 | 5.31 | 28.43 |
| F5I6P | 7.72 | 6.06 | 21.50 | 68.16 | 62.41 | 8.43 |
| G9L0P | 20.97 | 15.52 | 25.98 | 94.42 | 90.69 | 3.95 |
| F7J0P | 45.17 | 38.79 | 14.12 | 165.60 | 153.52 | 7.29 |
| F7J1P | 31.25 | 34.51 | 10.43 | 151.28 | 120.21 | 20.53 |
| G4K8P | 26.52 | 23.85 | 10.06 | 94.54 | 123.04 | 15.54 |
| G1K8P | 23.97 | 18.87 | 21.27 | 98.08 | 80.07 | 21.18 |
| G7K8P | 15.57 | 14.94 | 4.04 | 65.09 | 60.86 | 1.50 |
| G4I3M | 44.31 | 32.45 | 26.70 | 131.36 | 110.86 | 17.77 |
| TE-OA | 18.32 | 15.69 | 14.35 | 158.92 | 131.09 | 15.17 |
| TE-OBS | 23.51 | 25.53 | 8.59 | 71.82 | 72.90 | 12.90 |
| TE-OJP | 9.86 | 10.55 | 3.55 | 51.25 | 42.14 | 12.14 |
| TF-YJP | 8.87 | 7.88 | 2.88 | 15.22 | 12.91 | 4.91 |
| *RMS* Error % | 5.24 | | | 10.09 | | |

Table 6. Performance comparison of AIRSAR channles in estimating crown and stem biomass of BOREAS sites.
The accuracy estimated are calculated by comparing the results from each polarization combination with the field measured biomass values.

| *AIRSAR Channels* | *Crown Biomass Accuracy* | *Stem Biomass Accuracy* | *Total Biomass Accuracy* |
|---|---|---|---|
| PHH, PHV, LHV, CHV | 95% | 90% | 91% |
| PHH, PHV, PVV | 76% | 92% | 89% |
| LHH, LHV, LVV | 93% | 86% | 87% |
| CHH,CHV,CVV | 56% | 23% | 32% |
| LHH,CHH,CVV | 68% | 65% | 63% |

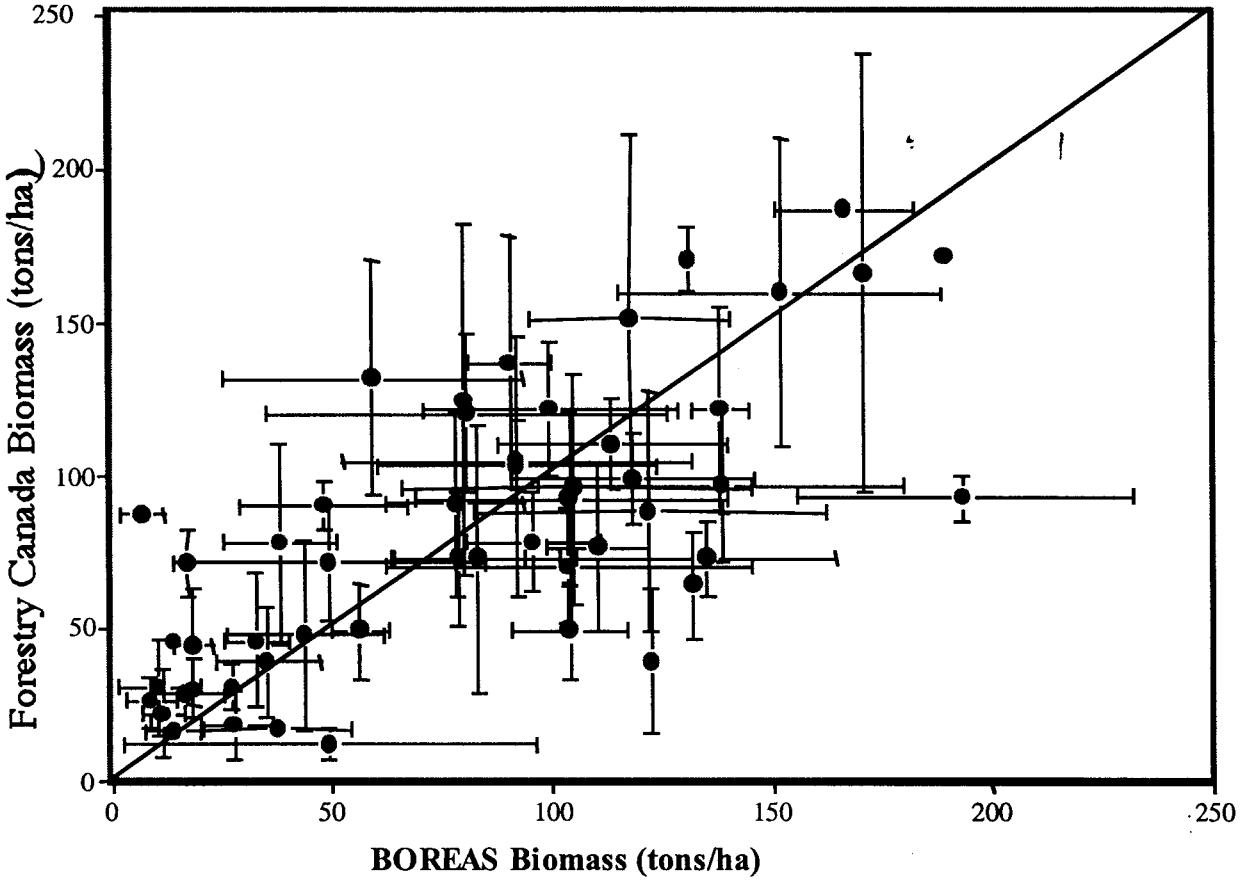
250
200
150
100
50
0
Forestry Canada Biomass (tons/ha)
0
50
100
150
200
250
BOREAS Biomass (tons/ha)

Figure 1

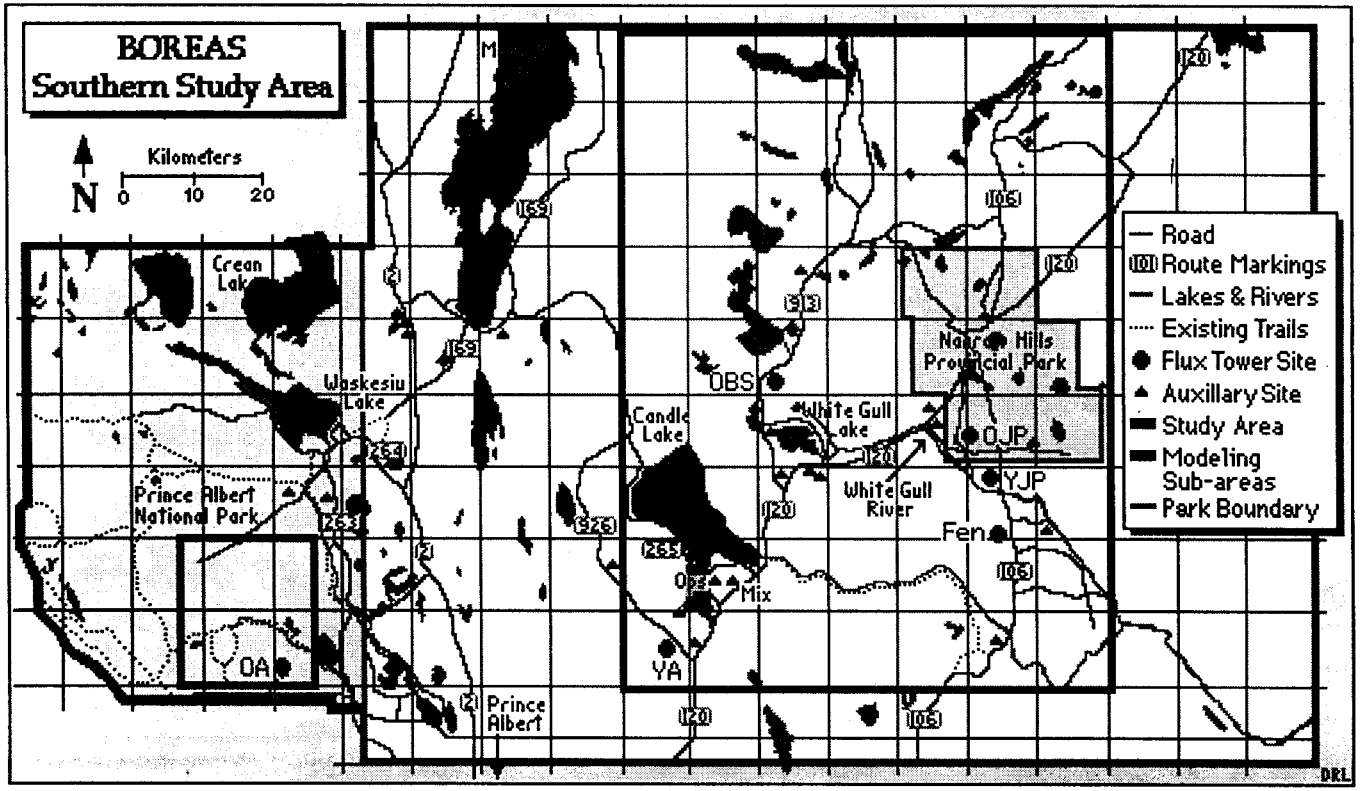
BOREAS
Southern Study Area
N
Kilometers
0 10 20
Crean Lake
Waskesiu Lake
Prince Albert National Park
OA
Prince Albert
Candle Lake
OBS
White Gull Lake
White Gull River
OJP
YJP
Fen
Mix
YA
Road
Route Markings
Lakes & Rivers
Existing Trails
Flux Tower Site
Auxillary Site
Study Area
Modeling Sub-areas
Park Boundary
DRL

Figure 2.

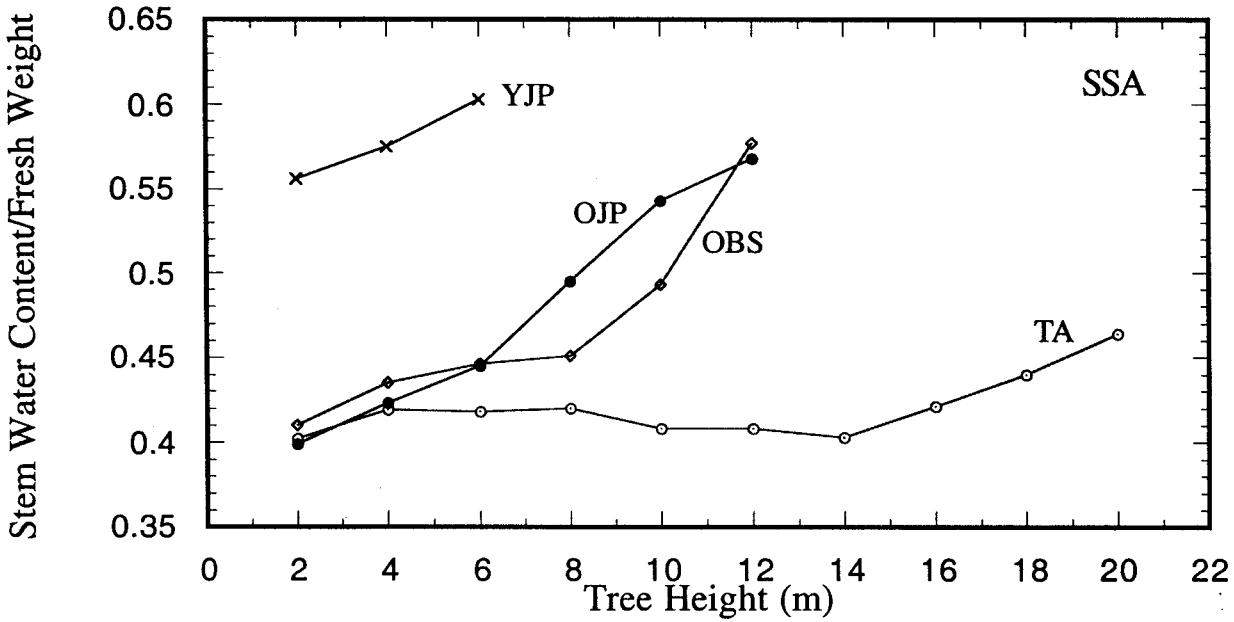
Stem Water Content/Fresh Weight
0.65
0.6
0.55
0.5
0.45
0.4
0.35
YJP
SSA
OJP
OBS
TA
0
2
4
6
8
10
12
14
16
18
20
22
Tree Height (m)

Figure 3.

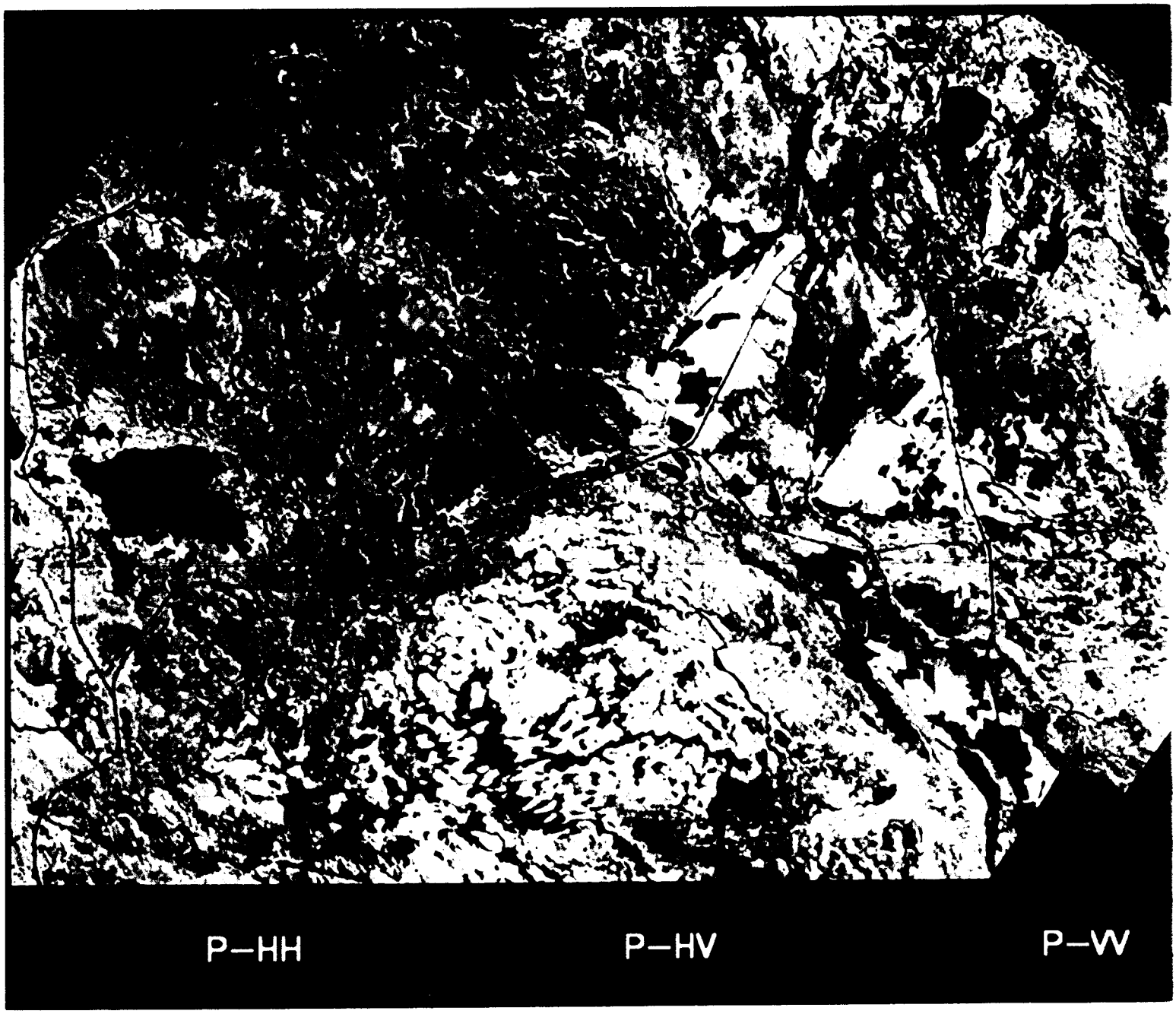


Figure 4.

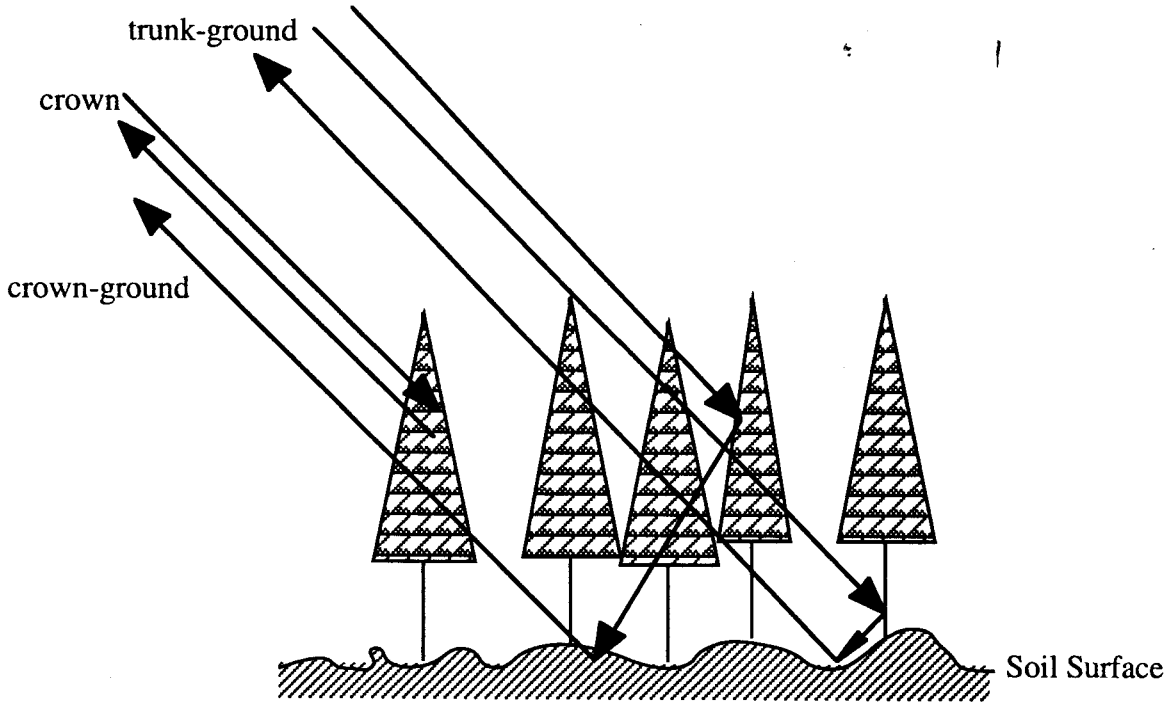


Figure 5.

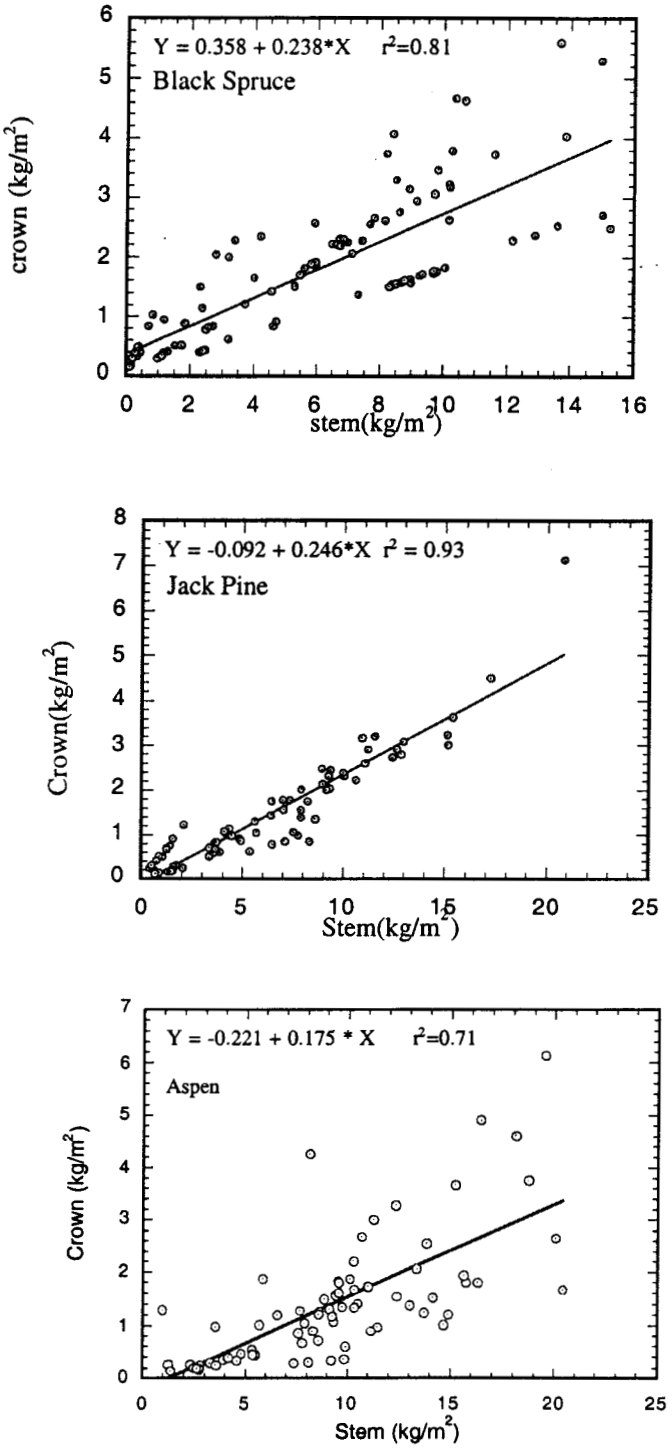
Y = 0.358 + 0.238*X r²=0.81
Black Spruce
crown (kg/m²)
stem(kg/m²)
Y = -0.092 + 0.246*X r² = 0.93
Jack Pine
Crown(kg/m²)
Stem(kg/m²)
Y = -0.221 + 0.175 * X r²=0.71
Aspen
Crown (kg/m²)
Stem (kg/m²)

Figure 6.

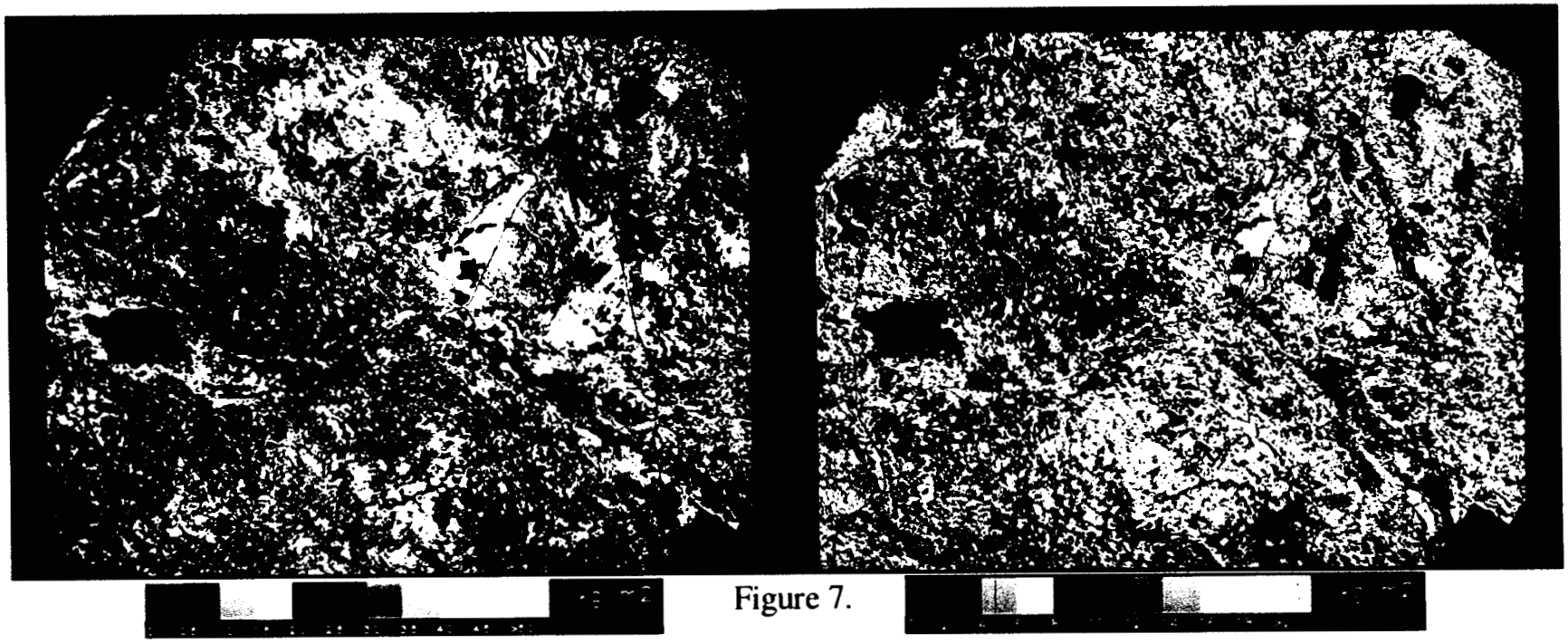

Figure 7.